Journal of Building Engineering 75 (2023) 106987

Contents lists available at ScienceDirect

Journal of Building Engineering

journal homepage: www.elsevier.com/locate/jobe

Reducing cement consumption in mortars by waste-derived hydrochars

Michael M. Santos [a, b], Antonio Luis Marques Sierra [c], Álvaro Amado-Fierro [a], Marta Suárez [d], Francisco Blanco [c], José Manuel González La Fuente [e], María A. Diez [a], Teresa A. Centeno [a, *]

[a] Instituto de Ciencia y Tecnología del Carbono (INCAR), CSIC, Francisco Pintado Fe 26, 33011, Oviedo, Spain
[b] Centre of Materials and Building Technologies (C–MADE/UBI), Department of Civil Engineering and Architecture, University of Beira Interior (UBI), 6201-001, Covilhã, Portugal
[c] Grupo de Modelización Matemática Aplicada (MOMA). Laboratorio de Tecnología de Cementos y Hormigones. Escuela de Ingeniería de Minas, Energía y Materiales de Oviedo, c/ Independencia 13, 33004, Oviedo, Spain
[d] Centro de Investigación en Nanomateriales Y Nanotecnología, Consejo Superior de Investigaciones Científicas (CSIC) - Universidad de Oviedo (UO) - Principado de Asturias, Avenida de la Vega 4, 6, El Entrego, 33940, San Martin del Rey Aurelio, Asturias, Spain
[e] R&D, COGERSA SAU, Carretera de Cogersa 1125, 33697, Gijón, Spain

ARTICLE INFO

Keywords:
Hydrothermal carbonization
Blended mortar
Mixed-municipal waste
Rice husk
Bio-waste recovery

ABSTRACT

Waste-derived hydrochars are presented for the first time as promising materials to reduce the consumption of natural resources and the carbon footprint of the cement industry, while eliminating waste and sequestering a high amount of carbon in civil infrastructures. Rice husk (RH) and stabilized organic waste from a mixed municipal waste mechanical-biological treatment plant (SOW) were subjected to hydrothermal carbonization at 200 °C for 2 h and the resulting hydrochars were thoroughly evaluated as cement substitutes in fresh and hardened mortars. Compared to the control, mortars with 1.25–5 wt% of cement replaced by hydrochar from stabilized organic fraction caused a decrease in compressive strength of about 50–60% at 28 days of curing, while flexural strength was diminished by about 38–47%. The use of rice husk-derived hydrochar led to a reduction of 32–47% in compressive strength and of 22–34% in flexural strength. With compressive and flexural strengths of 27–41 and 3.31–4.92 MPa, respectively, blended mortars (28 days) display good prospects for use in plastering, rendering, masonry, partition panels and low-load paving. On the other hand, substituting 5 wt% of cement by hydrochar decreases the thermal conductivity and increases electrical resistivity of the mortar by 25–30%, which enhances thermal insulation properties and potential durability. This approach opens a new avenue for large-scale application of biowaste hydrochars as secondary raw materials for sustainable construction.

1. Introduction

One of the most urgent challenges facing today's society is to manage efficiently and sustainably the huge amount of wastes generated daily. Traditional technologies, such as landfilling and even waste-to-energy by incineration, must be replaced to meet both the

* Corresponding author.
E-mail address: teresa.centeno@csic.es (T.A. Centeno).

https://doi.org/10.1016/j.jobe.2023.106987
Received 21 February 2023; Received in revised form 25 May 2023; Accepted 31 May 2023
Available online 1 June 2023

Sustainable Development Goals (SDGs) and the European hierarchy on waste that encourages material recovery. The targets of Directives 2018/850 and 2018/851 call for reducing landfilling to levels of ≤10% and increasing recycling to ≥65% by 2035, respectively.

In parallel, global production sectors need to make major efforts to minimize the greenhouse gas emissions (GHG) and the intensive use of natural resources [1]. One of the productive segments most concerned with sustainability worldwide is the construction industry. Recent estimates indicate that around 10% of the total anthropogenic CO_2 emissions and 6% of GHG come from the cement industry [2,3] and the high demand for new constructions in recent years only increases concerns about the intensification of emissions and consumption of energy and raw materials [4].

Along with the deployment of innovative technologies [5], circular economy approaches, and the development of alternative binders [6] to replace the globally dominant lime-based Portland cement, one promising strategy to mitigate the carbon footprint is the incorporation of efficient and sustainable supplementary cementing materials (SCM) into the production cycle. This explains the current boost of research on a wide variety of materials, such as cenospheres, slag, fly ash [7], biomass ash [8], marble and granite dust [3], graphene nanoparticles [9], etc., to be used as SCM.

Several studies have addressed biomass as a suitable candidate for partial cement replacement, but several adverse effects hinder its direct application in mortar and concrete [10,11]. Among other factors, the low cement-biomass compatibility, the instability of the biomass in the alkaline cement matrix and the high water absorption significantly deteriorate the properties of the resulting cementitious materials. Biomass tends to segregate and float on the surface of the paste, so its homogeneous distribution in the cement matrix is a current challenge. On the other hand, the increase in temperature generated by the reaction of the cement with the water and the alkalinity of the hydrated cement favour the dissolution of low molecular weight carbohydrates and some degradation of the more stable biopolymers, which causes dimensional changes in the biomass and an increase in the amount of soluble carbohydrates with aging. In addition, the mineralization processes that certain types of biomass undergo due to the presence of Ca^{2+} or other cations in the cement suspension increase the embrittlement of mortar and concrete. Another aspect to consider is that sugars and, to a lesser extent, hemicellulose, cellulose and lignin can contribute to the inhibition of cement hydration and delay or shorten the setting time of cement. Furthermore, the absorption of water leads to a continuous volume change of the biomass within the cement matrix, causing interfacial damage and inducing concrete cracking. Likewise, the addition of biomass leads to an increase in shrinkage due to the loss of free water. No less relevant drawback is the high variation in the properties of natural materials, making it difficult to predict the properties of the final products.

As a low-cost alternative, biochar, which is obtained by subjecting biomass to high temperatures of 300–650 °C in the absence or limited supply of oxygen, is attracting considerable attention due to some promising attributes. Although biochar encompasses a wide variety of features depending on the precursor and the synthesis procedure, it is generally characterized by high carbon storage and chemical stability, low thermal conductivity and flammability, and a relatively well-developed porous structure [12]. Diverse biochars derived from a variety of organic wastes have proved successful admixtures in cementitious materials [11–17]. The porosity and surface chemistry rich in functional groups have been reported to facilitate good interaction with the cementitious matrix and biochar can potentially be used as a low density material for more energy efficient and less dense composites. The addition of biochar may enhance the mechanical properties of cementitious materials, acting as an internal water reservoir that promotes secondary hydration and additional curing. On the other hand, nano/micro-particles of biochar could serve as a filler to reduce the porosity and, consequently, water permeability in composite products. It has been found that the improvement in resistance is highly dependent on the precursor and process conditions used for biochar production [18].

As a consequence of the great variability in the intrinsic characteristics of different biochars, there is no ideal biochar/cement ratio. In general, the substitution of up to 5% of cement by biochar favours the performance of the resulting composites, but above 5–7% may reduce the mechanical properties with respect to the plain mortar. However, some studies reported that dosages of over 10–20 wt% reduce the composite density, while compressive and flexural strengths are enhanced. On the other hand, 2–8% cement replacement increases water absorption and capillary porosity and decreases water penetration due to saturation [19].

The morphology and size of the particles, the content of carbon, oxygen, volatile matter and ash, as well as pores volume and pores size distribution largely determine how biochar interacts with the cementitious matrix, leading to more or less promising results [11–17,19].

Compared to standard pyrolysis leading to biochar, hydrothermal carbonization (HTC) is an innovative technology that eliminates the pre-drying step and takes place at lower temperature, which implies less energy consumption. It is performed in the presence of water at temperatures of 180–250 °C under the autogenous saturation vapor pressure of water at the reaction temperature. Subcritical water acts as a reagent that increases the solubility of organic compounds and facilitates subsequent reactions to transform the organic feedstock into a stable carbon-enriched solid (the so-called hydrochar) [20–24] On the other hand, HTC improves the carbonaceous solid yield (50–80 wt%), the liquid by-product (25–55 wt%) can be valorized within a circular economy framework, and the gases given off represent only 5–10 wt%.

Economic studies [25,26] estimate a current price for hydrochar at around 150–200 €/Tn, although it is expected to become significantly cheaper as HTC technological progresses will increase the capacity to treat larger quantities of biomass in a more efficient way. Moreover, the use of certain wastes will bring additional credit by avoiding the management costs. The final value of hydrochar in the market will depend on several factors, such as demand, competing materials or incentives for use.

Several studies have reported the attributes of hydrochars for diverse applications, such as biofuels, soil amendments, catalyst support, adsorbents, supercapacitors, particleboards, etc. [22,24,27–30]. Going one step further, this research addresses for the first time the hydrochar potential in cementitious materials and shows that the production of secondary raw materials by HTC is a promising route for organic waste valorization. Hydrochar for mortar presents interesting prospects for a large market. The closure of conven-

tional coal-fired power plants will lead to a shortage of fly ash in the medium term, and materials derived from biomass will be in great demand as part of the ongoing decarbonization process.

The mechanical-biological treatment (MBT) is a globally extended technology that aims to recover materials and reduce the discharge of mixed municipal waste. Despite the sorting process, the stabilized organic fraction (SOW) contains significant amounts of glass, plastic, metals, etc., and cannot be considered as compost under EU Regulation 2019/1009. Moreover, its high ash content prevents its energy use. Therefore, SOW remains a problematic stream mainly dedicated to landfill-covering purposes or, even worse, is directly discharged in landfills [31]. In this context, it is a priority to find innovative applications to fit this waste into an efficient and low carbon economy.

On the other hand, current world rice production exceeds 700 million tons and the husk, which represents about 20% by weight, is considered an interesting material for construction due to the relevant presence of silica [32]. Numerous studies have explored rice husk ash to replace part of the cement in mortars. However, doubts are raised about the effectiveness of this approach in terms of the high environmental damage and the limited efficiency of the uncontrolled burning process. More recently, investigations on the use of rice husk-biochar [33,34] have been encouraged on the basis of the lower impact of its production, but the emission of tar and gases is still very high. It is worth trying a more sustainable treatment such as HTC for the recovery of this waste.

This paper focuses on the characteristics of the resulting hydrochars and the properties of composite mortars resulting from the substitution of 1.25–5 wt% of cement by these carbonaceous materials. Systematic comparison of blended mortars, both fresh and hardened, allows a critical evaluation of the suitability of hydrochar as a secondary raw material in sustainable construction by acting as a carbon sink.

2. Materials and methods

For the sake of clarity, Scheme 1 summarises the experimental design followed in this study. The details of the methodology and protocols used are given below.

2.1. Raw materials

Stabilized organic fraction from mechanical-biological treatment of mixed-municipal waste (SOW) supplied by COGERSA (www.cogersa.es) and rice husk (RH) provided by DACSA (www.dacsa.com) were used as feedstocks for HTC treatment.

As summarized in Table 1, SOW is characterized by a moisture of 48.9 wt% and an inorganic fraction content as high as 35.5 wt%. The volatile matter accounts for 59.1 wt%, the fixed carbon being limited to 5.4 wt%. Rice husk moisture does not surpass 11.3 wt%

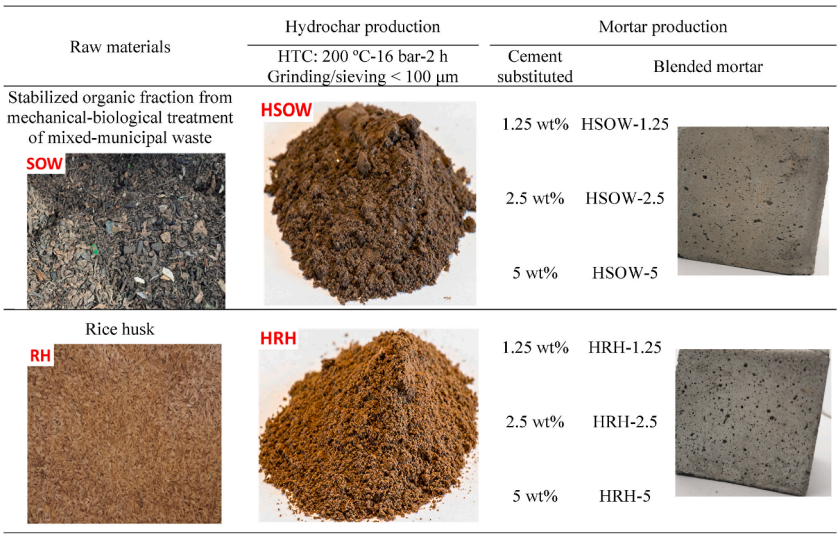

Scheme 1. Experimental design.

Table 1
Chemical characteristics of biomass wastes and hydrochars.

Sample	Yield (wt.% d.b.)	Proximate analysis (wt.% d.b.)			Ultimate analysis (wt.% d.b.)					Atomic ratio	
		Ash	Volatile Matter	Fixed Carbon	C	H	N	S	O	O/C	H/C
SOW	–	35.5	59.1	5.4	34.9	4.2	1.9	0.5	23.0	0.49	1.44
HSOW	71.8	42.8	48.9	8.3	32.9	3.8	1.1	0.4	19.0	0.43	1.39
RH	–	12.5	69.6	17.9	44.1	5.4	0.5	0.1	37.4	0.64	1.47
HRH	72.2	15.7	61.6	22.7	47.1	5.0	0.6	0.1	31.5	0.50	1.27

and the ash and volatile matter contents are 12.5 and 69.6 wt%, respectively. The presence of fixed carbon in RH is nearly 18 wt% (Table 1). Both residues present O/C and H/C atomic ratios within the typical ranges reported for biomass [35], although the O/C value is significantly higher for the rice husk than for the stabilized organic fraction.

For the mortar production, Portland cement CEM I 52.5 N (Table A1) was utilized conforming to NP EN 197-1 and RP 15.01 AENOR. It was combined with CEN Standard Sand with specific grain size distribution between 0.08 and 2 mm (UNE-EN 196-1:2018 (EN 196-1:2016)), at least 98% SiO_2 content and 0.2 wt% of maximum moisture.

2.2. Hydrochar synthesis

Representative samples of the bio-wastes SOW and RH were mixed with water in a ratio of 1:4 by weight (including the moisture content of the feedstock) and then heated in a 3 L ILSHIN stainless steel jacketed pressure reactor at 200 °C for 2 h under autogenous pressure of ~16 bar. The resulting hydrochar was air-dried in an oven at 105 °C for 24 h and, finally, ground and sieved below 100 μm (Scheme 1). To guarantee the sample representativeness, 3 batches with 1 kg of SOW/run and 5 batches with 250 g of RH/run were prepared. The hydrochars are labelled as HSOW and HRH, respectively. The process yield was calculated by Y (%) = [mass of dry hydrochar/mass of dry feedstock] × 100.

2.3. Characterization of feedstocks and hydrochars

Moisture and ash contents were evaluated according to ASTM7582 in a LECO TGA70 and a muffle furnace was used to quantify the volatile matter (ISO 562:2010). The fixed carbon was calculated by difference (FC = 100-[moisture]-[ash]-[volatile matter]).

The hydrochar samples were burnt at 815 °C and the composition of the ashes was assessed by X-ray fluorescence (SRS 3000-Bruker spectrometer), the elements being expressed as typical oxides. The main mineralogical phases present in the hydrochars were identified by X-ray diffraction (AXS D8 Advanced-Bruker diffractometer). The C, H, N and S content (ASTM D5373 and ASTM D4239) was determined by a LECO TruSpec Micro analyzer, estimating the percentage of O from [O] = 100-[ash]-[C]-[H]-[N]-[S].

Thermogravimetric tests were performed under N_2 flow (75 mL/min) from 30 °C to 1000 °C (20 °C/min) with a holding time of 5 min (Mettler TG-DSC1 Star system).

A Nicolet IR 8700 Fourier transform infrared spectrometer (FTIR) with a Smart Collector diffuse reflectance accessory (DRIFT) was used to analyze the superficial functional groups. A high-sensitivity mercury-cadmium telluride detector (MCT-A) cooled by liquid nitrogen was used and 64 scans at 4 cm^{-1} resolution were accumulated in the middle spectral range of 4000-650 cm^{-1}.

Particle size distribution was determined using a laser diffraction particle size analyzer (Beckman Coulter LS-13-320). Field Emission Scanning Electron Microscopy (FESEM) observations were accomplished by using a Carl Zeiss DMS-942 microscope.

Skeletal density was estimated by He pycnometry (Micromeritics AccuPyC 1330). Bulk density and pore size distribution were determined by Hg intrusion in the pressure range of 0.005–228 MPa (Micromeritics Autopore IV 9500). The porosity assessment was complemented with N_2 physisorption at 77 K (Micromeritics ASAP 2010). Prior to textural characterization, hydrochars and cement were degassed at 50 °C and 105 °C, respectively, for 16 h under vacuum.

Following the NF P 18–513 standard, the Chapelle test was used as a direct methodology to evaluate the pozzolanic activity of hydrochars (see details in Appendix A, Fig. A1).

2.4. Production of mortars

According to UNE-EN 196-1:2018, the reference mortar was obtained with a mixture of 450 (±2) g of cement, 1350 (±5) g of sand and 225 (±1) g of water. For the blended mortars, the hydrochar was included in the binder replacing 1.25, 2.5 and 5 wt% of the cement. The fresh mortar was prepared by mechanical mixing (ICON Horizontal Mixer (Investigaciones de la CONstrucción) and compacted in two layers, each with 60 blows, using a mold with three horizontal compartments and a standard compactor (ICON Horizontal Compactor (Investigaciones de la CONstrucción). The mold containing the specimens was kept in a humid chamber at 20 ± 1 °C and relative humidity ≥90 wt% for 24 h. The specimens were then demolded and immediately immersed in water (20.0 ± 1.0 °C) until strength tests were performed at 7, 14, 28 and 90 days. The hydrochar-bearing mortars are identified by the name of the hydrochar followed by the percentage of cement substituted.

Details of the preparation, shaping and curing of the mortars is illustrated in Fig. A2.

2.5. Mortars characterization

The consistency of the fresh mortars was estimated with an ICON shaking table (Investigaciones de la CONstrucción) and following the standard UNE-EN 1015-3:2000 (EN 1015-3:1999). The bulk density was evaluated according to UNE-EN 1015-6:1999 (EN 1015-6:1998). The setting time (±10 min) was determined from the average value of three simultaneous determinations by the Vicat test (UNE-EN 196-3:2017 (EN 196-3:2016)). The trial was carried out in an Ibertest Auto-Vicat connected to an Acer Aspire E1-572-G laptop with VICATEST software. The expansion accompanying the cement hydration process was evaluated using the Le-Chatelier test (UNE-EN 196-3:2017).

The microstructure of the hardened mortars at 28 days was observed by FESEM (Carl Zeiss DMS-942 microscope) and their skeletal and bulk densities were assessed by He pycnometry (Micromeritics AccuPyC 1330) and Hg intrusion at 0.1013 MPa (Micromeritics Autopore IV 9500), respectively. Hg intrusion from 0.005 MPa to 228 MPa provided insight into porosity features. The samples were previously degassed at 105 °C under vacuum for 16 h.

Probes of 40 mm × 40 mm × 160 mm (UNE-EN 196-1: 2018) cured for 7, 14 and 28 days were subjected to mechanical compression (500 N/s) and flexural (50 N/s) tests in a METROTEST series DMD 200 kNa. The thermal conductivity of 28-day mortars was estimated by a Meter TEMPOS thermal properties analyzer (ASTM D5334-00:2011). The electrical resistivity was assessed as indi-

cated by UNE 83988-1:2008 (equivalent to EN 12390-19:2023). A Koban KM-05 and Palm Size UT131 series multimeters and a Wanptek NSP1203W 0/120V/3A power supply were used.

Pictures of the systems used for testing hydrochar-based mortars are shown in Fig. A2.

The statistical analysis of the data by RStudio [36] has focused on a descriptive statistics study evaluating the mean value of the variables together with the standard deviation.

3. Results and discussion

3.1. Hydrochar characteristics

Without the pre-drying required for standard thermochemical conversion of biomass, the stabilized organic fraction from MBT and rice husk are successfully transformed into carbonaceous solids by a simple hydrothermal treatment at 200 °C for only 2 h. The yield about 72 wt% of hydrochar (Table 1) clearly competes with the <50 wt% biochar usually obtained by dry pyrolysis of these feedstocks at 450–800 °C [37,38].

The profiles obtained by thermogravimetric analysis (Fig. 1a and b) reveal that hydrothermal carbonization partially removes the most thermally unstable bio-components, whereas those remaining degrade at higher temperature.

HTC facilitates the decomposition and solubilization of biopolymers at a temperature as low as 200 °C [20–22] and, consequently, the resulting solids contain less volatile matter than the respective crude wastes.

Proximate analysis confirms the decrease in volatile species and the increase in the fixed carbon after HTC (Table 1). The inorganic fraction (ash) is also concentrated in both hydrochars, accounting for 42.8 wt% for HSOW and 15.7 wt% for HRH. As shown in Table 2, SOW contains oxides similar to those in cement (Table A1) and hydrothermal treatment enhances their presence in the resulting solid, with the exception of K_2O and Na_2O. Rice husk has a significant content of SiO_2, which is also increased after HTC.

The amount of silica present in both hydrochars (~20 wt% for HSOW and ~15 wt% for HRH) is promising for valorization in mortars. SiO_2 is necessary for the production of hydrated calcium silicate gel with cementitious properties, although it is required to be in a non-crystalline state. The XRD spectra (Fig. A3) illustrate that crystalline and amorphous phases coexist in the hydrochar HSOW, with calcite, quartz and sodium aluminum silicate being the main crystalline compounds detected. In contrast, amorphous phases are dominant in the rice husk-derived material.

The lower O/C and H/C atomic ratios in hydrochars than in their feedstocks (Table 1) reflect the predominant dehydration and deoxygenation reactions promoted by HTC in organic materials [39], although their extent is rather limited due to the gentle conditions

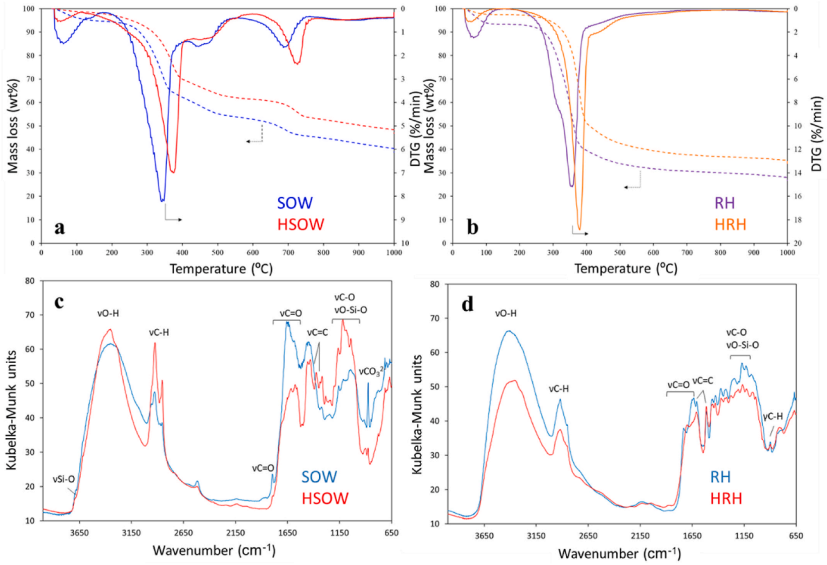

Fig. 1. TG and DTG curves (a,b) and Fourier-transform infrared spectra (c,d) of stabilized organic waste (SOW) and rice husk (RH) and the corresponding hydrochars (HSOW and HRH).

Table 2
Modification of waste ash composition with the HTC process and the Chapelle index of hydrochars.

Sample	SiO_2 (wt.% d.b.)	Fe_2O_3 (wt.% d.b.)	Al_2O_3 (wt.% d.b.)	CaO (wt.% d.b.)	K_2O (wt.% d.b.)	Na_2O (wt.% d.b.)	MgO (wt.% d.b.)	Chapelle index (%)
SOW	15.60	0.99	2.12	9.27	1.02	1.51	1.55	–
HSOW	19.80	1.37	3.08	11.28	0.56	0.98	1.84	28
RH	11.57	0.01	<0.001	0.15	0.49	<0.001	0.08	–
HRH	15.44	0.04	<0.001	0.13	0.02	<0.001	<0.001	43

of the present treatment. For comparison, the O/C and H/C ratios of biochars produced from municipal solid waste (MSW) at 300–700 °C are in the ranges 0.25-0.05 and 1.19-0.30, respectively [37]. For rice husk-biochars prepared at 350–800 °C, Bushra and Remya [38] report values of 0.56-0.03 for O/C and 0.61-0.35 for H/C.

It is worth noting that the solids HSOW and HRH obtained by fast, low-energy HTC successfully retain 68 wt% and 77 wt% of the carbon initially existing in the raw wastes. These values far exceed the carbon recovery capacity displayed by biochars produced at 500 °C from MSW (40 wt%) [37] and rice husk (48 wt%) [38].

Fourier-transform infrared spectra (Fig. 1c and d) indicate that the main changes experienced by the SOW surface after HTC include the increase in aliphatic groups (especially in CH_2 groups, nearly at 2920 and 2850 cm^{-1}) and the decrease in oxygenated functionalities, such as O-H (broad band at 3350 cm^{-1}), anhydride (1795 cm^{-1}), carboxyl (1700 cm^{-1}) and carbonyl (1656 cm^{-1}) groups. An increasing intensity of the bands associated to $\nu C=O$ (1704 cm^{-1}), $\nu C\text{-}O$ (1316 cm^{-1}) and $\nu O\text{-}H$ (1431 cm^{-1}) reflects a greater presence of carboxylic groups. In addition, HTC on SOW also provokes the removal of calcium carbonate as indicated by intensity decrease of the distinctive very-sharp band at 874 cm^{-1}. The concentration of mineral species in silicates (3600 and 1200-1000 cm^{-1}) also takes place.

The surface of the rice husk and its hydrochar (Fig. 1d) contains similar functional groups, including O-H, C-H in aliphatic, C=O, C=C and C-O groups, and those of silica species (Si-O-Si, Si-H and Si-OH bonds). The changes in the primary C=O functionalities after HTC treatment of RH are mostly due to the cleavage of the functional groups of hemicelluloses and lignin, i.e., the C=O in the unconjugated and conjugated systems (decrease of the prominent bands centered at nearly 1735 and 1650 cm^{-1}, respectively), the transformation of the pristine ester groups to carboxyl groups (new band at ~1700 cm^{-1}), and the decrease in the 898 cm^{-1} band attributed to C-H deformation in polysaccharides. In addition, the HRH spectrum shows an increase in the band intensity at nearly 1515 cm^{-1} attributed to the aromatic C=C of lignin, suggesting a higher level of carbohydrate degradation.

After grinding, the hydrochars have a particle size distribution similar to that of cement (Fig. 2a), but FESEM reveals different morphology (Fig. A4). In contrast to the spherical regularity of the cement particles, those of HSOW and HRH are irregular, predominantly elongated and fibrillar for the former, whereas some of the latter have a spongy appearance.

The hydrochars display some porous development (Fig. 2b and Fig. A5) with a total pore volume of 0.71 $cm^3\ g^{-1}$ for HSOW and 0.91 $cm^3\ g^{-1}$ for HRH. In agreement with the absence of significant narrow porosity reported by N_2 physisorption (Fig. A6), mercury porosimetry reveals an essentially open network composed of large cavities (Fig. 2b). The higher pore volume of rice husk-hydrochar (Fig. 2b-inset) is consistent with its lower density (Table A2). The larger pores (Fig. 2b) of HRH results in a total specific surface area of 19.5 $m^2\ g^{-1}$ against 25.6 $m^2\ g^{-1}$ displayed by HSOW (Table A2).

3.2. Pozzolanic behavior of hydrochars

The Chapelle test indicates that both HSOW and HRH display ability to react with calcium hydroxide in the presence of water and promote additional formation of secondary calcium silicate hydrate gel in cementitious matrix. Rice husk-derived hydrochar shows a Chapelle Index (CI) of 43.1%, reaching the limit of 330 mg CaO g^{-1} required for materials classified as pozzolans [40]. The pozzolanic activity of HRH is consistent with the presence of reactive amorphous silica (Fig. A3) [41], which successfully participates in further hydration reactions. In the case of HSOW, despite a higher SiO_2 + Al_2O_3 + Fe_2O_3 content (Table 2), its pozzolanic behavior (CI = 28.3%) seems to be penalized by the crystalline nature of the inorganic compounds (Fig. A3), mainly from quartz [41]. Nevertheless, it should be noted that the consumption of 216.3 mg CaO g^{-1} when hydrochar from the stabilized organic waste is included in the mortar is higher than the amount achieved with eucalyptus bark ash and comparable to biomass ash and some metakaolins [42].

3.3. Mortar performance

3.3.1. Fresh state

3.3.1.1. Water requirement and consistency. As reported for the mortars with biochar [16], the replacement of cement by rice husk-hydrochar implies a higher water requirement in the binder to achieve the desired consistency. It is often argued that the specific

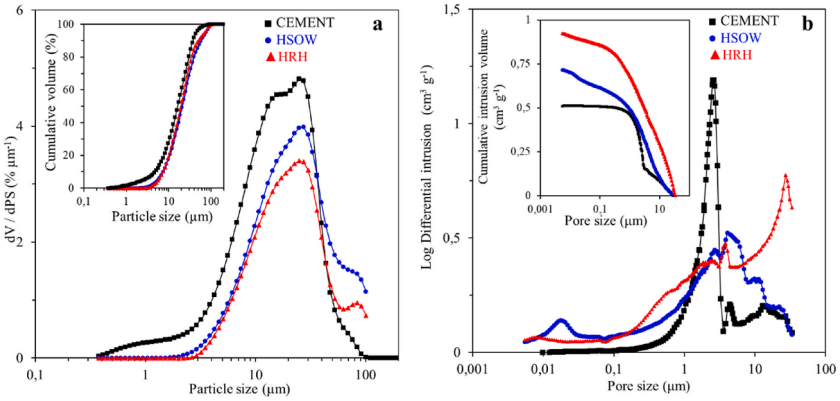

Fig. 2. Particle size distribution [inset-cumulative volume] (a) and pore size distribution [inset-total pore volume] (b) of hydrochars and cement.

surface area derived from a highly developed microporous structure is responsible for the ability of biochars to absorb water when processed in mortar [15,43], but this is not straightforwardly applicable to hydrochars. Thus, the inclusion of HRH as substitute of 1.25, 2.5 and 5 wt% cement increases the water requirement by 3, 5 and 8%, respectively. Although HSOW has a higher specific surface area than HRH (Table A2), the mixture HSOW-1.25 does not need more water than the plain mortar, and by increasing the substitution rate to 2.5 and 5 wt%, the water requirement is only 1 and 3 wt% higher.

In the case of hydrochars, rather than the specific surface area, the key seems to be in the oxygen functionalities present on their surface, which provide a high affinity for water through the formation of hydrogen bonds [43,44]. Along with higher pore volume, the HRH surface contains greater density of [O]-functionalities (its total O content is 1.7 times higher than in HSOW (Table 1)), thus providing more active centers for water holding.

The relevant capacity of HRH to absorb water is confirmed by a simple test in which 1 g of dry hydrochar is placed in contact with 10 g of water for 2 h. It is found that the material experiences an increase of 121.6 wt%, while the increment for HSOW is limited to 49.3 wt%. As comparison, water absorption capacity of cement under the same experimental conditions is 29.7 wt%.

The incorporation of 1.25% of HSOW results in a slightly higher flowability (Table 3), which may be due to a combination with water favored by the replacement of a fraction of cement particles by larger hydrochar particles. This effect seems to be compensated by the water absorption capacity of HSOW when the dosage is increased to 2.5 wt%. For a 5 wt% replacement, the latter predominates and a reduction in the workability of the composite mortar HSOW-5 is observed.

In the case of the addition of rice husk-hydrochar, the flowability decreases for all substitution rates, which is consistent with less free water available as a consequence of the highly hydrophilic nature of the HRH surface.

This behavior is in line with the general trend of loss of workability reported for fresh mortars containing biochar [15,16,45,46], which can be compensated to some extent by incorporating a superplasticizer into the mix [16,45].

3.3.1.2. Density. Table 3 illustrates that the presence of hydrochar at different dosages also influences the fresh density of composite mortars. The decrease in density may be due to the partial replacement of cement by less dense materials [15]. However, no direct relationship is found between the present hydrochars density and that of the corresponding mortars. Although HSOW is denser than HRH, its incorporation at 1.25–5 wt% dosage causes a reduction of 11–19% with respect to the density of the control. When rice husk-hydrochar is used as substitute, the decrease is less marked, being limited to 8–11%. This suggests that other factors such as shape, roughness and porosity of the particles and affinity for water can play a role. As observed for mortars including biochar with different water absorption capacity, the lower density of the composite with HSOW is attributed to a higher volume of free water in the fresh cement paste due to the lower absorption capacity of the hydrochar derived from the stabilized organic fraction [15].

3.3.1.3. Setting times. Studies with geopolymer mortars [47,48] showed that cement substitution implies a lower tricalcium aluminate content leading to a delay in mortar curing. On the contrary, Gupta et al. [49] reported that the incorporation of biochar in mortar mixes reduces initial and final setting times as its particles act as nucleation sites for cement hydration.

For the hydrochars studied here, the setting time is not appreciably affected when 1.25 wt% cement is replaced by HSOW or HRH and remains around the 150 min required for plain mortar (Fig. 3).

In contrast, the onset and end of setting are delayed with increasing dosage, and the retardation degree is highly dependent on the type of hydrochar. The incorporation of 2.5% and 5% hydrochar derived from stabilized organic wastes increases the setting time to 170 min (HSOW-2.5) and 200 min (HSOW-5), respectively (Fig. 3a). The same percentages of rice husk-hydrochar cause the setting time to rise to 180 min for HRH-2.5 and reach 290 min for HRH-5 (Fig. 3b). According to Chen et al. [50], the more notable delay generated by HRH may be due to the higher density of oxygenated functional groups (especially carboxyl and hydroxyl functionalities) on its surface.

3.3.1.4. Le-Chatelier soundness. The excessive volume expansion of the mortar that sometimes accompanies cement hydration is responsible for the appearance of cracks, distortions and disintegrations that compromise the durability of the final products [51]. Le Chatelier's method indicates that the expansion of mixtures containing 1.25–5 wt% of HRH and HSOW does not exceed 1%. Hydrochar, with its ability to retain water, acts as an internal source of water to fill the porosity created by chemical shrinkage, thus hindering the generation of meniscus and tensile forces and, consequently, reducing autogenous shrinkage [52]. The poor formation of expansive phases, such as ettringite, reduces the risk of internal stresses, cracking and degradation of the cement matrix with a positive impact on the service life and performance of the mortar or concrete.

Table 3
Characteristics of fresh and hardened mortars.

Sample	Fresh mortar		Hardened mortar (28-days)			
	Consistency (mm)	Bulk density (g cm^{-3})	Skeletal density (g cm^{-3})	Bulk density (g cm^{-3})	Thermal conductivity (W m^{-1} K^{-1})	Electrical resistivity (kΩ-cm)
Control	119 ± 2	2.22 ± 0.01	2.44 ± 0.01	2.16 ± 0.01	1.66 ± 0.03	6.12 ± 0.01
HSOW-1.25	128 ± 2	1.97 ± 0.03	2.37 ± 0.02	1.89 ± 0.02	1.34 ± 0.02	5.13 ± 0.01
HSOW-2.5	119 ± 5	1.85 ± 0.02	2.39 ± 0.03	1.90 ± 0.03	1.26 ± 0.03	4.52 ± 0.02
HSOW-5	109 ± 3	1.80 ± 0.02	2.39 ± 0.01	1.90 ± 0.02	1.40 ± 0.02	4.22 ± 0.01
HRH-1.25	115 ± 6	2.04 ± 0.06	2.38 ± 0.02	2.07 ± 0.02	1.25 ± 0.02	5.12 ± 0.03
HRH-2.5	106 ± 2	2.01 ± 0.02	2.38 ± 0.01	2.00 ± 0.03	1.23 ± 0.02	4.98 ± 0.01
HRH-5	88 ± 2	1.97 ± 0.01	2.37 ± 0.02	1.95 ± 0.03	1.15 ± 0.01	4.56 ± 0.01

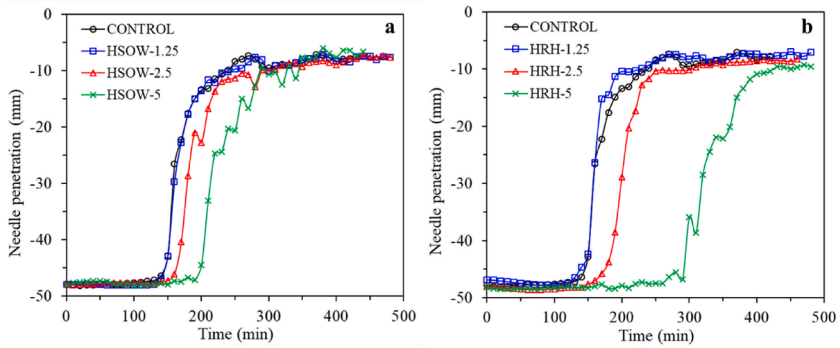

Fig. 3. Setting time for percentage replacement of cement by hydrochars from stabilized organic waste (a) and from rice husk (b).

3.3.2. Hardened mortar

3.3.2.1. Microstructure. The microstructure was studied on the cross section of the fractured mortars (Fig. A7). The FESEM image of the mortar with 1.25 wt% of hydrochar from stabilized organic residue (HSOW-1.25) at 28 days (Fig. 4) clearly reveals the presence of portlandite plates (1) and needle-shaped amorphous hydrated calcium silicate (2). The latter is one of the main hydration products of Portland cement and is responsible for setting and hardening. It is formed by a dissolution-precipitation process during the reaction with water of the main constituents of Portland cement, tricalcium silicate (Ca_3SiO_5) and β-dicalcium silicate (Ca_2SiO_4), but also by the reaction of silica and lime in water (the so-called pozzolanic reaction). Since it does not have a well-defined stoichiometry ($CaO\text{-}SiO_2\text{-}H_2O$), it is usually represented as C-S-H [53].

The larger fibrillar structures correspond to C-S-H gels (3) [54], and the globular structures most likely derive from the transformation of portlandite into C-S-H honeycomb. Hardly any portlandite is identified in the mortar with 2.5 wt% HSOW (Fig. A8), but the presence of C-S-H gels in the form of elongated filaments and needles is easily detected. The C-S-H honeycomb is predominant in the case of 5 wt% substitution of cement.

With respect to the mortars including rice husk-hydrochar, HRH-1.25 shows an appreciable amount of portlandite bound by fibrillar C-S-H gel bridges (4) and dispersed needle items of C-S-H (5) between the portlandite crystals (Fig. 4). Where the cement substitution reaches 2.5 and 5 wt% (Fig. A8), broad C-S-H honeycomb structures and a lower presence of fibrillar C-S-H gels are observed. Portlandite plates appear sporadically.

The cross section of mortar without hydrochar used as control (Fig. 4) reveals portlandite plates (6), fibrillar structures of C-S-H gels (7) and globular C-S-H structures (8).

3.3.2.2. Density and porosity. Regardless of the type and dosage of hydrochar incorporated into the paste, the skeletal density of the hardened mortar changes only slightly, from 2.44 to 2.39–2.37 g cm^{-3} (Table 3). However, as observed for the fresh mortar, hydrochar induces a reduction in the bulk density of the dry mortar.

Fig. 5 shows that composite mortars contain random porosity distributed into gel pores, capillary pores, mesopores, and air pores [55]. As a general pattern, the replacement of cement by hydrochar leads to some development of gel pores, a shift of capillary pores to smaller sizes, the creation of a significant amount of mesopores, as well as a less significant generation of air pores. More specifically, the porosity of the mortar doubles with the addition of the stabilized organic waste-hydrochar, and all mortars containing HSOW show a total pore volume of 0.12–0.13 $cm^3\ g^{-1}$ (Fig. 5a). Their total pore area is around 7.2–7.9 $m^2\ g^{-1}$, while that of the plain mortar is 4.3 $m^2\ g^{-1}$. Fig. 5b illustrates that all HSOW dosages generate a similar pore size distribution in the mortar, the most relevant change being the creation of mesopores in the range of 0.2–10 μm with a maximum around 1–2 μm. In contrast, a progressive increment in pore volume and mesopore creation are observed with the amount of cement replaced by HRH (Fig. 5c), the maximum corresponding to 0.105 $cm^3\ g^{-1}$ (8.1 $m^2\ g^{-1}$) with a broad peak around 1.5 μm clearly visible for 5 wt% substituted (Fig. 5d).

The fact that the densification of the mortar achieved with biochar is not detected when hydrochar is incorporated (Table 3) may be due to the lower porosity of hydrochar and therefore lower water adsorption capacity. On the other hand, it is likely that a filling

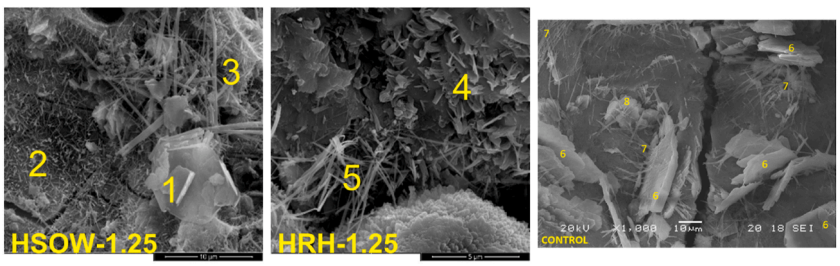

Fig. 4. FESEM images of the cross section of the fractured mortars with 1.25 wt% cement substituted by hydrochars HSOW and HRH (28 days ageing). Control is included for comparison.

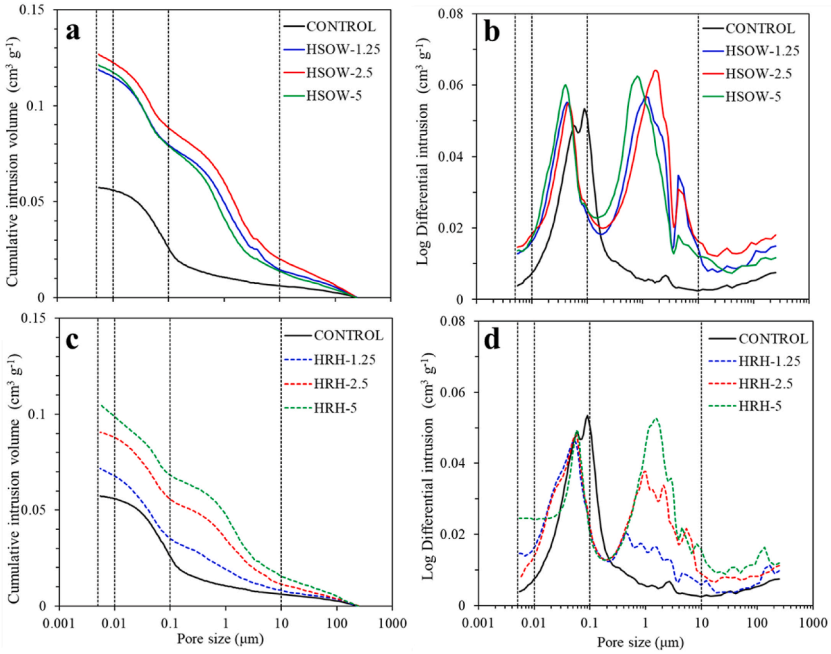

Fig. 5. Cumulative pore volume and pores size distribution of mortars with hydrochar doses of stabilized organic wastes (a,b) and rice husk (c,d) at 28 days.

effect can be achieved by using a finer fraction of hydrochar particles compared to cement particles. As has been reported for biochar [11], an increase in the packing density of the mixture can be obtained by filling the voids between the cement and sand grains. This effect would also increase the water-holding capacity of the hydrochar, leading to better cohesion of the mix and reduced bleeding, which would shorten the setting time.

3.3.2.3. Mechanical properties. Fig. 6 illustrates the modification of the compressive and flexural strength of mortars with the hydrochar dosage and the curing time. Table A3 reports relatively low standard deviation values, indicating little dispersion in the sample space analysed.

It is observed that the partial replacement of cement by hydrochar leads to a significant reduction in the compressive strength of mortars (Fig. 6a,c). Compared to the control, the compressive strength of the mortar mixed with stabilized organic fraction hydrochar drops by around 50–60%. Although less relevant, the reduction remains around 32–47% when hydrochar derived from rice husk is used as cement substitute.

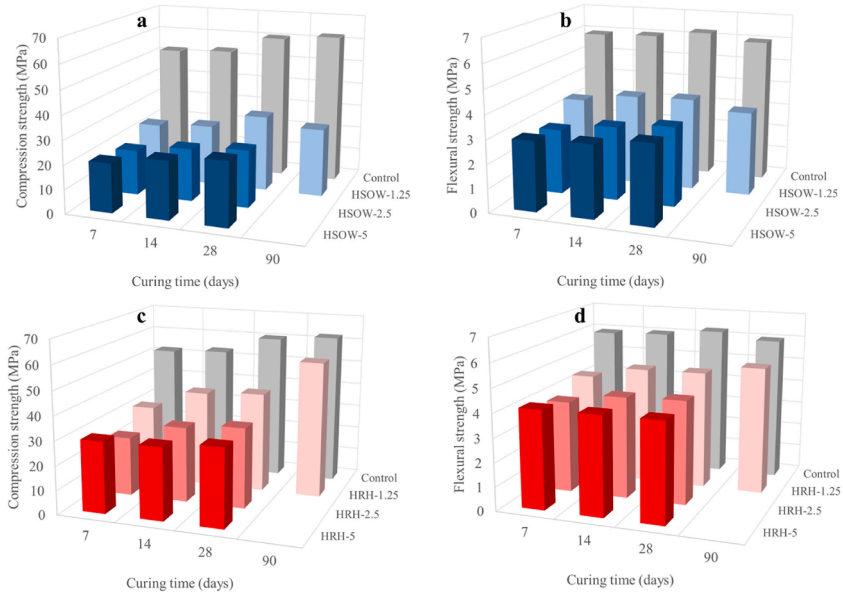

Fig. 6. Evolution of the compressive and flexural strength of mortars with the hydrochar dosage and the curing time.

The presence of hydrochar has a smaller effect on the flexural strength (Fig. 6b,d), the decrease being around 38–47% for the HSOW hydrochar and 22–34% for HRH.

On one hand, this is a consequence of the so-called dilution effect [56], since the generation of hydration products (such as C-S-C) important for the strength of cementitious composites is decreased. On the other hand, to the extent that mortar strength is also negatively related to its pore volume (Fig. A9), HSOW-mortars result penalized by their more porous structure (Fig. 5).

It is observed that the strength partially recovers for longer curing stages (Fig. 6). The pozzolan HRH favors the formation of additional C-S-H gels (section 3.2), which can also fill some capillary spaces, thus improving the system strength. This reaction seems to proceed slowly, as suggested by the remarkable increment in the compressive strength of HRH-1.25 after 90-days ageing. Taking the value at 90 days as a reference, the control and the mortar containing 1.25 wt% HSOW reaches 83% of the maximum compression strength over the first 7 days, but that with the same dose of rice husk-hydrochar shows a clear delay. It only achieves 56% of the maximum strength at 7-days and does not even exceed 74% after 28 days of maturation. At higher dosages, the mortar strength tends to decrease, although the reduction is not proportional to the amount of cement substituted (Fig. 6) and the values with 2.5 and 5 wt% of hydrochars are quite similar.

The behavior of mortars composed of hydrochar is quite different from the usual performance of those that include biochar. Thus, the addition of biochar at low doses of 1–2 wt% as a substitute of cement improves compressive strength [57], while it is reduced at higher dosages [12]. The high porosity of biochar favours water retention during the mixing phase, which subsequently promotes secondary hydration reactions and further curing, leading to improved mechanical properties. The absorption capacity of biochar generates a lower proportion of binder and a densified microstructure is produced. Furthermore, it has been indicated that the ability of biochar nanoparticles (<6 μm) to fill the pores also improves the mechanical properties. On the other hand, the strength reduction for higher dosages is due to the dilution effect of the biochar in the cement, which leads to a limited production of calcium silicate hydrate.

According to the standards UNE-EN 998-1:2018 (EN 998-1:2016) and UNE-EN 998-2:2018 (EN 998-2:2016), the mechanical strengths of these composites far exceed the values required for mortars used in plastering, rendering and masonry. They also display great potential for application in partition blocks, low-traffic parking lots, bike paths, local streets and pedestrian areas [58–60]. As has been reported for biochar-containing mortars, further improvements can be achieved by adapting the physicochemical characteristics and size/shape of hydrochar particles and by adjusting the dosage [11,12,14,49].

3.3.2.4. Thermal conductivity. The substitution of 1.25–5 wt% cement by hydrochars HSOW and HRH successfully contributes to the reduction of the thermal conductivity of the mortar. Thus, the mortar with 5 wt% of cement replaced by HRH shows a thermal conductivity 31% lower than that of plain mortar (Table 3) and 2.5% HSOW allows a reduction of 25%. The decrease of this parameter with the density of hardened mortars indicates that the development of porosity driven by the presence of hydrochar facilitates the disruption of thermal bridging within the cementitious composites [12,14], improving the thermal insulation performance.

Reduced thermal conductivity means less thermal stresses in the mortar subjected to temperature changes, which reduces the risk of cracking and degradation and can help prevent accelerated degradation of the mortar and structure in the event of fire.

3.3.2.5. Electrical resistivity. The degradation processes affecting the mortars are partially controlled by the transport of ions from the hydration solution through the microstructure. They cause degradation of the cement matrix and corrosion of reinforcement, compromising the mortar stability and the integrity of the structure. The correlation found between electrical resistivity and diffusion and migration of chloride [61,62] and sulfate [62] ions means that this parameter can be used indirectly as a reliable indicator of the potential durability of mortars and concretes in harsh environments (i.e. coastal areas) [63,64].

The gradual descend of the electrical conductivity of mortars shown in Table 3 reveals that the presence of hydrochar results to be advantageous. A cement substitution rate of 1.25 wt% leads to a 16% reduction, whereas the 25–31% decrease achieved with 5 wt% indicates better durability prospects for composites with high doses of hydrochar. Attending to the increased porosity development in the blended mortars, this evolution suggests a reduction in pore connectivity and/or changes in the ionic concentrations of the pore fluid as a consequence of the hydrochar presence.

4. Conclusions

Without pre-drying, hydrothermal carbonization at 200 °C and 16 bar for 2 h successfully transforms rice husk and stabilized organic waste from MBT plant into 72 wt% of hydrochar that effectively retains 77-68% of the initial carbon.

Beyond the typical energy or soil amendment applications addressed so far for hydrochars, this study shows that they also have potential for implementation as a partial substitute for cement in mortars. This opens a new avenue that represents an opportunity to increase the profitability of hydrothermal carbonization, in terms of large-scale efficient recycling of residual biomass to produce secondary raw materials for more sustainable construction within low-carbon economy.

In general, the substitution of 1.25–5% by weight of cement by hydrochars derived from the stabilized organic fraction of MBT plant and rice husk delays the setting time and reduces the density of the resulting mortars.

One of the drawbacks associated to the presence of hydrochars is the notable development of pores in the range of 0.2–10 μm with a maximum around 1–2 μm, which entails a relevant reduction in mechanical properties. A drop in compressive strength of 32–60% and flexural strength of 22–47% after 28 days of curing limits the application of these composite mortars to non-structural systems. However, their compressive strength of 27–41 MPa holds great promise for plastering, masonry, partition walls and low-load paving.

As a positive impact of the 5 wt% replacement of cement by hydrochar, it is worth highlighting the reduction in thermal conductivity and the increase in electrical resistivity. Quantitative changes of the order of 25–30% for both parameters suggest significant improvements in thermal insulation and durability for the blended mortars.

The results obtained here encourage further exploration of hydrochars prepared from other types of raw materials and under various HTC conditions. Based on these operational aspects, the potential market for the final product and the benefits in terms of environmental sustainability and public health, an economic analysis will provide insights into the global profitability.

Author contributions

Michael M. Santos: Conceptualization, Methodology, Investigation, Writing - original draft.
Antonio Luis Marques Sierra: Conceptualization, Investigation, Methodology, Writing - Review & Editing.
Álvaro Amado-Fierro: Investigation, writing - original draft.
Marta Suárez: Investigation, writing - original draft.
Francisco Blanco: Conceptualization, Supervision, Investigation.
José Manuel González: Conceptualization, Resources, Writing - Review & Editing.
Maria A. Diez: Investigation, Writing - Review & Editing.
Teresa A. Centeno: Conceptualization, Funding acquisition, Investigation, Methodology, Resources, Supervision, Writing - Review & Editing.

Declaration of competing interest

The authors declare that they have no known competing financial interests or personal relationships that could have appeared to influence the work reported in this paper.

Data availability

No data was used for the research described in the article.

Acknowledgments

Funding from the European Regional Development Fund (ERDF) through project CEMOWAS^2 (SOE2/P5/F0505)-INTERREG V SUDOE 2017 and from the Plan de Ciencia, Tecnología e Innovación (PCTI) 2018-2022 del Principado de Asturias and the ERDF (project IDI/2021/000037) is gratefully acknowledged. CINN acknowledges the financial support received from FICYT (IDI/2021/000106). Michael M. Santos thanks the University of Beira Interior and the Spanish National Research Council (CSIC) for the Erasmus + internship award. This study was carried out with the support of COGERSA for obtaining and managing the SOW sample and of the company DACSA for supplying the rice husk. The assistance of the INCAR-CSIC library service led by Luis Gutiérrez Fernández-Tresguerres is highly appreciated.

Appendix A. Supplementary data

Supplementary data to this article can be found online at https://doi.org/10.1016/j.jobe.2023.106987.

References

[1] https://www.eea.europa.eu/en/topics, 2023.
[2] I.N. York, I. Europe, Concrete needs to lose its colossal carbon footprint, Nature 597 (2021) 593–594, https://doi.org/10.1038/d41586-021-02612-5.
[3] A. Danish, M.A. Mosaberpanah, M.U. Salim, R. Fediuk, M.F. Rashid, R.M. Waqas, Reusing marble and granite dust as cement replacement in cementitious composites: a review on sustainability benefits and critical challenges, J. Build. Eng. 44 (2021) 102600, https://doi.org/10.1016/j.jobe.2021.102600.
[4] O. Heinz, H. Heinz, Cement interfaces: current understanding, challenges, and opportunities, Langmuir 37 (2021) 6347–6356, https://doi.org/10.1021/acs.langmuir.1c00617.
[5] P.S. Fennell, S.J. Davis, A. Mohammed, Decarbonizing cement production, Joule 5 (2021) 1305–1311, https://doi.org/10.1016/j.joule.2021.04.011.
[6] G. Fahim Huseien, J. Mirza, M. Ismail, S.K. Ghoshal, A. Abdulameer Hussein, Geopolymer mortars as sustainable repair material: a comprehensive review, Renew. Sustain. Energy Rev. 80 (2017) 54–74, https://doi.org/10.1016/j.rser.2017.05.076.
[7] A. Danish, M.A. Mosaberpanah, Influence of cenospheres and fly ash on the mechanical and durability properties of high-performance cement mortar under different curing regimes, Construct. Build. Mater. 279 (2021) 122458, https://doi.org/10.1016/j.conbuildmat.2021.122458.
[8] A.L. Yadav, V. Sairam, L. Muruganandam, K. Srinivasan, An overview of the influences of mechanical and chemical processing on sugarcane bagasse ash characterisation as a supplementary cementitious material, J. Clean. Prod. 245 (2020) 118854, https://doi.org/10.1016/j.jclepro.2019.118854.
[9] R. Alves e Silva, P. de Castro Guetti, M.S. da Luz, F. Rouxinol, R.V. Gelamo, Enhanced properties of cement mortars with multilayer graphene nanoparticles, Construct. Build. Mater. 149 (2017) 378–385, https://doi.org/10.1016/j.conbuildmat.2017.05.146.
[10] L.T.T. Vo, P. Navard, Treatments of plant biomass for cementitious building materials – a review, Construct. Build. Mater. 121 (2016) 161–176, https://doi.org/10.1016/j.conbuildmat.2016.05.125.
[11] A. Danish, M. Ali Mosaberpanah, M. Usama Salim, N. Ahmad, F. Ahmad, A. Ahmad, Reusing biochar as a filler or cement replacement material in cementitious composites: a review, Construct. Build. Mater. 300 (2021) 124295, https://doi.org/10.1016/j.conbuildmat.2021.124295.
[12] B.A. Akinyemi, A. Adesina, Recent advancements in the use of biochar for cementitious applications: a review, J. Build. Eng. 32 (2020) 101705, https://doi.org/10.1016/j.jobe.2020.101705.
[13] H. Maljaee, H. Paiva, R. Madadi, L.A.C. Tarelho, M. Morais, V.M. Ferreira, Effect of cement partial substitution by waste-based biochar in mortars properties, Construct. Build. Mater. 301 (2021) 124074, https://doi.org/10.1016/j.conbuildmat.2021.124074.
[14] H. Maljaee, R. Madadi, H. Paiva, L. Tarelho, V.M. Ferreira, Incorporation of biochar in cementitious materials: a roadmap of biochar selection, Construct. Build. Mater. 283 (2021) 122757, https://doi.org/10.1016/j.conbuildmat.2021.122757.
[15] S. Gupta, H.W. Kua, H.J. Koh, Application of biochar from food and wood waste as green admixture for cement mortar, Sci. Total Environ. (2018) 619–620 https://doi.org/10.1016/j.scitotenv.2017.11.044, 419–435.
[16] S. Gupta, H.W. Kua, S.D. Pang, Biochar-mortar composite: manufacturing, evaluation of physical properties and economic viability, Construct. Build. Mater. 167 (2018) 874–889, https://doi.org/10.1016/j.conbuildmat.2018.02.104.
[17] R.A. Mensah, V. Shanmugam, S. Narayanan, S.M.J. Razavi, A. Ulfberg, T. Blanksvärd, F. Sayahi, P. Simonsson, B. Reinke, M. Försth, G. Sas, D. Sas, O. Das,

Biochar-added cementitious materials—a review on mechanical, thermal, and environmental properties, Sustain. Times 13 (2021) 1–27, https://doi.org/10.3390/su13169336.
[18] I. Cosentino, L. Restuccia, G.A. Ferro, J.M. Tulliani, Type of materials, pyrolysis conditions, carbon content and size dimensions: the parameters that influence the mechanical properties of biochar cement-based composites, Theor. Appl. Fract. Mech. 103 (2019) 102261, https://doi.org/10.1016/j.tafmec.2019.102261.
[19] J.R. Nahuat-Sansores, J.C. Cruz, M.P. Gurrola, D. Trejo-Arroyo, Suitability of biochar as supplementary cementitious material (SCM) or filler: waste revalorization, a critical review, J. Civ. Eng. 6 (2022) 12–31, https://doi.org/10.35429/JCE.2022.16.6.12.31.
[20] A. Funke, F. Ziegler, Hydrothermal carbonization of biomass: a summary and discussion of chemical mechanisms for process engineering, Biofuels, Bioprod. Biorefining. 4 (2010) 160–177, https://doi.org/10.1002/bbb.198.
[21] A. Kumar, K. Saini, T. Bhaskar, Hydochar and biochar: production, physicochemical properties and techno-economic analysis, Bioresour. Technol. 310 (2020) 123442, https://doi.org/10.1016/j.biortech.2020.123442.
[22] H.S. Kambo, A. Dutta, A comparative review of biochar and hydrochar in terms of production, physico-chemical properties and applications, Renew. Sustain. Energy Rev. 45 (2015) 359–378, https://doi.org/10.1016/j.rser.2015.01.050.
[23] X. Zhuang, J. Liu, Q. Zhang, C. Wang, H. Zhan, L. Ma, A review on the utilization of industrial biowaste via hydrothermal carbonization, Renew. Sustain. Energy Rev. 154 (2022) 111877, https://doi.org/10.1016/j.rser.2021.111877.
[24] A. Khosravi, H. Zheng, Q. Liu, M. Hashemi, Y. Tang, B. Xing, Production and characterization of hydrochars and their application in soil improvement and environmental remediation, Chem. Eng. J. 430 (2022) 133142, https://doi.org/10.1016/j.cej.2021.133142.
[25] D. Sangaré, M. Moscosa-Santillan, A. Aragón Piña, S. Bostyn, V. Belandria, I. Gökalp, Hydrothermal carbonization of biomass: experimental study, energy balance, process simulation, design, and techno-economic analysis, Biomass Convers. Biorefinery (2022), https://doi.org/10.1007/s13399-022-02484-3.
[26] M. Lucian, L. Fiori, Hydrothermal carbonization of waste biomass: process design, modeling, energy efficiency and cost analysis, Energies 10 (2017) 1–18, https://doi.org/10.3390/en10020211.
[27] M.M. Santos, M.A. Diez, M. Suárez, T.A. Centeno, Innovative particleboard material from the organic fraction of municipal solid waste, J. Build. Eng. 44 (2021) 103375, https://doi.org/10.1016/j.jobe.2021.103375.
[28] Z. Zhang, Z. Zhu, B. Shen, L. Liu, Insights into biochar and hydrochar production and applications: a review, Energy 171 (2019) 581–598, https://doi.org/10.1016/j.energy.2019.01.035.
[29] L. Suárez, I. Benavente-Ferraces, C. Plaza, S. de Pascual-Teresa, I. Suárez-Ruiz, T.A. Centeno, Hydrothermal carbonization as a sustainable strategy for integral valorisation of apple waste, Bioresour. Technol. 309 (2020) 123395, https://doi.org/10.1016/j.biortech.2020.123395.
[30] L. Guardia, L. Suárez, N. Querejeta, C. Pevida, T.A. Centeno, Winery wastes as precursors of sustainable porous carbons for environmental applications, J. Clean. Prod. 193 (2018) 614–624, https://doi.org/10.1016/J.JCLEPRO.2018.05.085.
[31] K. Bernat, I. Wojnowska-baryła, M. Zaborowska, I. Samul, Insight into the composition of the stabilized residual from a full-scale mechanical-biological treatment (MBT) plant in terms of the potential recycling and recovery of its contaminants, Sustain. Times 13 (2021) 1–16, https://doi.org/10.3390/su13105432.
[32] M. Amran, R. Fediuk, G. Murali, N. Vatin, M. Karelina, T. Ozbakkaloglu, R.S. Krishna, A.S. Kumar, D.S. Kumar, J. Mishra, Rice husk ash-based concrete composites: a critical review of their properties and applications, Crystals 11 (2021) 1–33, https://doi.org/10.3390/cryst11020168.
[33] Z. Asadi Zeidabadi, S. Bakhtiari, H. Abbaslou, A.R. Ghanizadeh, Synthesis, characterization and evaluation of biochar from agricultural waste biomass for use in building materials, Construct. Build. Mater. 181 (2018) 301–308, https://doi.org/10.1016/j.conbuildmat.2018.05.271.
[34] S. Muthukrishnan, S. Gupta, H.W. Kua, Application of rice husk biochar and thermally treated low silica rice husk ash to improve physical properties of cement mortar, Theor. Appl. Fract. Mech. 104 (2019) 102376, https://doi.org/10.1016/j.tafmec.2019.102376.
[35] D.W. van Krevelen, Coal:Typology – Chemistry –Physics – Constitution, 3th edition, Elsevier, Amsterdam, 1993.
[36] RStudio Team, RStudio, Integrated Development for R. RStudio, PBC, Boston, MA, 2020 URL. http://www.rstudio.com.
[37] R. Zornoza, F. Moreno-Barriga, J.A. Acosta, M.A. Muñoz, A. Faz, Stability, nutrient availability and hydrophobicity of biochars derived from manure, crop residues, and municipal solid waste for their use as soil amendments, Chemosphere 144 (2016) 122–130, https://doi.org/10.1016/j.chemosphere.2015.08.046.
[38] B. Bushra, N. Remya, Biochar from pyrolysis of rice husk biomass—characteristics, modification and environmental application, Biomass Convers. Biorefinery (2020) 7–12, https://doi.org/10.1007/s13399-020-01092-3.
[39] J.A. Libra, K.S. Ro, C. Kammann, A. Funke, N.D. Berge, Y. Neubauer, M.M. Titirici, C. Fühner, O. Bens, J. Kern, K.H. Emmerich, Hydrothermal carbonization of biomass residuals: a comparative review of the chemistry, processes and applications of wet and dry pyrolysis, Biofuels 2 (2011) 71–106, https://doi.org/10.4155/bfs.10.81.
[40] A.L. Borges, S.M. Soares, T.O.G. Freitas, A.O. Junior, E.B. Ferreira, F.G.S. Ferreira, Evaluation of the pozzolanic activity of glass powder in three maximum grain sizes, Mater. Res. 24 (2021), https://doi.org/10.1590/1980-5373-MR-2020-0496.
[41] M. Frías, H. Savastano, E. Villar, M.I. Sánchez De Rojas, S. Santos, Characterization and properties of blended cement matrices containing activated bamboo leaf wastes, Cem. Concr. Compos. 34 (2012) 1019–1023, https://doi.org/10.1016/j.cemconcomp.2012.05.005.
[42] J. Pontes, A. Santos Silva, P. Faria, Evaluation of pozzolanic reactivity of artificial pozzolans, Mater. Sci. Forum 730–732 (2013) 433–438. https://doi.org/10.4028/www.scientific.net/MSF.730-732.433.
[43] Q. Ren, Z. Zeng, Z. Jiang, Q. Chen, Incorporation of bamboo charcoal for cement-based humidity adsorption material, Construct. Build. Mater. 215 (2019) 244–251, https://doi.org/10.1016/j.conbuildmat.2019.04.173.
[44] T. Han, Application of peanut biochar as admixture in cement mortar, IOP Conf. Ser. Earth Environ. Sci. 531 (2020) 012061, https://doi.org/10.1088/1755-1315/531/1/012061.
[45] A. Sirico, P. Bernardi, B. Belletti, A. Malcevschi, E. Dalcanale, I. Domenichelli, P. Fornoni, E. Moretti, Mechanical characterization of cement-based materials containing biochar from gasification, Construct. Build. Mater. 246 (2020) 118490, https://doi.org/10.1016/j.conbuildmat.2020.118490.
[46] A.N. Ofori-Boadu, R. Kelley, F. Aryeetey, E. Fini, P. Akangah, The influence of swine-waste biochar on the early-age characteristics of cement paste, Int. J. Eng. Res. Afr. 7 (2017) 1–7, https://doi.org/10.9790/9622-0706010107.
[47] H.E. Elyamany, A.E.M. Abd Elmoaty, A.M. Elshaboury, Setting time and 7-day strength of geopolymer mortar with various binders, Construct. Build. Mater. 187 (2018) 974–983, https://doi.org/10.1016/j.conbuildmat.2018.08.025.
[48] A.B. Malkawi, M.F. Nuruddin, A. Fauzi, H. Almattarneh, B.S. Mohammed, Effects of alkaline solution on properties of the HCFA geopolymer mortars, Procedia Eng. 148 (2016) 710–717, https://doi.org/10.1016/j.proeng.2016.06.581.
[49] S. Gupta, H.W. Kua, C.Y. Low, Use of biochar as carbon sequestering additive in cement mortar, Cem. Concr. Compos. 87 (2018) 110–129, https://doi.org/10.1016/j.cemconcomp.2017.12.009.
[50] X. Chen, M.G. Matar, D.N. Beatty, W.V. Srubar, Retardation of Portland cement hydration with photosynthetic algal biomass, ACS Sustain. Chem. Eng. 9 (2021) 13726–13734, https://doi.org/10.1021/acssuschemeng.1c04033.
[51] S. Sharma, Experimental investigation of partial replacement of OPC (43 grade) cement by egg shell powder for M-35 concrete grade, J. Emerg. Technol. Innov. Res. 5 (2018) 1–9.
[52] P.C. Aïtcin, Phenomenology of Cement Hydration, Elsevier Ltd, 2016, https://doi.org/10.1016/B978-0-08-100693-1.00002-3.
[53] S. Garrault-Gauffinet, A. Nonat, Experimental investigation of calcium silicate hydrate (C-S-H) nucleation, J. Cryst. Growth 200 (1999) 565–574, https://doi.org/10.1016/S0022-0248(99)00051-2.
[54] L. Evangelista, M. Guedes, Microstructural studies on recycled aggregate concrete, new trends eco-efficient recycl, Concrete 24 (2018) 425–451, https://doi.org/10.1016/B978-0-08-102480-5.00014-2.
[55] Q. Ma, Y. Yu, M. Sindoro, A.G. Fane, R. Wang, H. Zhang, Carbon-based functional materials derived from waste for water remediation and energy storage, Adv. Mater. 29 (2017) 1605361, https://doi.org/10.1002/adma.201605361.
[56] F. Massazza, Pozzolanic cements, Cem. Concr. Compos. 15 (1993) 185–214, https://doi.org/10.1016/0958-9465(93)90023-3.
[57] L. Wang, L. Chen, D.C.W. Tsang, B. Guo, J. Yang, Z. Shen, D. Hou, Y.S. Ok, C.S. Poon, Biochar as green additives in cement-based composites with carbon dioxide curing, J. Clean. Prod. 258 (2020) 120678, https://doi.org/10.1016/j.jclepro.2020.120678.

[58] L. Wang, L. Chen, D.C.W. Tsang, H.W. Kua, J. Yang, Y.S. Ok, S. Ding, D. Hou, C.S. Poon, The roles of biochar as green admixture for sediment-based construction products, Cem. Concr. Compos. 104 (2019) 103348, https://doi.org/10.1016/j.cemconcomp.2019.103348.
[59] L. Wang, L. Chen, D.C.W. Tsang, J.S. Li, K. Baek, D. Hou, S. Ding, C.S. Poon, Recycling dredged sediment into fill materials, partition blocks, and paving blocks: technical and economic assessment, J. Clean. Prod. 199 (2018) 69–76, https://doi.org/10.1016/j.jclepro.2018.07.165.
[60] American Concrete Institute 330R-08, Guide for the Design and Construction of Concrete Parking Lots, 2008. www.concrete.org.
[61] K. Ram, M. Serdar, D. Londono-Zuluaga, K. Scrivener, The effect of pore microstructure on strength and chloride ingress in blended cement based on low kaolin clay, Case Stud. Constr. Mater. 17 (2022) e01242, https://doi.org/10.1016/j.cscm.2022.e01242.
[62] S. Gupta, S. Muthukrishnan, H.W. Kua, Comparing influence of inert biochar and silica rich biochar on cement mortar – hydration kinetics and durability under chloride and sulfate environment, Construct. Build. Mater. 268 (2021) 121142, https://doi.org/10.1016/j.conbuildmat.2020.121142.
[63] P. Azarsa, R. Gupta, Electrical resistivity of concrete for durability evaluation: a review, Adv. Mater. Sci. Eng. (2017) 1–30 https://doi.org/10.1155/2017/8453095, 2017.
[64] W.J. McCarter, G. Starrs, T.M. Chrisp, Electrical conductivity, diffusion, and permeability of Portland cement-based mortars, Cement Concr. Res. 30 (2000) 1395–1400, https://doi.org/10.1016/S0008-8846(00)00281-7.

Update

Journal of Building Engineering

Volume 80, Issue , 1 December 2023, Page

DOI: https://doi.org/10.1016/j.jobe.2023.108081

Journal of Building Engineering 80 (2023) 108081

Contents lists available at ScienceDirect

Journal of Building Engineering

journal homepage: www.elsevier.com/locate/jobe

Corrigendum to "Reducing cement consumption in mortars by waste-derived hydrochars" [J. Build. Eng. 75 (2023) 1–13 106987]

Michael M. Santos [a,b], Antonio Luis Marques Sierra [c], Álvaro Amado-Fierro [a], Marta Suárez [d], Francisco Blanco [c], José Manuel González La Fuente [e], María A. Diez [a], Teresa A. Centeno [a,*]

[a] *Instituto de Ciencia y Tecnología del Carbono (INCAR), CSIC, Francisco Pintado Fe 26, 33011, Oviedo, Spain*
[b] *Centre of Materials and Building Technologies (C–MADE/UBI), Department of Civil Engineering and Architecture, University of Beira Interior (UBI), 6201-001, Covilhã, Portugal*
[c] *Grupo de Modelización Matemática Aplicada (MOMA), Laboratorio de Tecnología de Cementos y Hormigones, Escuela de Ingeniería de Minas, Energía y Materiales de Oviedo, c/ Independencia 13, 33004, Oviedo, Spain*
[d] *Centro de Investigación en Nanomateriales Y Nanotecnología, Consejo Superior de Investigaciones Científicas (CSIC), Universidad de Oviedo (UO), Principado de Asturias, Avenida de la Vega 4, 6, El Entrego, 33940, San Martin del Rey Aurelio, Asturias, Spain*
[e] *R&D, COGERSA SAU, Carretera de Cogersa 1125, 33697, Gijón, Spain*

The authors regret to note that on page 7, in Table 3, the values shown in the last column correspond to electrical conductivity (S/cm) instead of electrical resistivity (kΩ-cm).

The authors would like to apologise for any inconvenience caused.

DOI of original article: https://doi.org/10.1016/j.jobe.2023.106987.

* Corresponding author. Instituto de Ciencia y Tecnología del Carbono (INCAR), CSIC, Francisco Pintado Fe 26, 33011, Oviedo, Spain.
E-mail address: teresa.centeno@csic.es (T.A. Centeno).

https://doi.org/10.1016/j.jobe.2023.108081

Available online 4 November 2023